In an actual tunnel, the finite thickness of the shear layer and of the wall boundary layers will make the situation even worse. Shear layers between two supersonic streams are known to have *positive* displacement thickness.[4] That, combined with the displacement thickness of the boundary layers will decrease the effective diffuser area. On the other hand, the present zero-growth assumption for the shear layer is not bad for a relatively short test section length, because supersonic shear layers grow extremely slowly compared to subsonic ones.[5] Obviously, the longer the channel, the more severe the viscous effects will be. Dutton et al.[6] found that if the channel length of a supersonic-supersonic ejector is very long, the flow inside the ejector may suffer a normal-shock-like deceleration, with an accompanying total pressure loss, static pressure rise, and Mach number decrease to subsonic values.

The second throat areas depicted on Fig. 3 correspond to steady-state, running conditions. They do not reflect the requirements for starting the tunnel. In one-stream tunnels, the minimum second throat area required for starting is considerably larger than that required for running, even under inviscid conditions. It is safe to assume that the same is true for two-stream tunnels, although their starting process is too complex to be addressed here. For $M_{1,\infty}$ and $M_{2,\infty}$ substantially different, the second throat provides minute pressure recovery (Figs. 2b and 2c) and introduces the risk of not being able to start. In that case, it appears best to eliminate the second throat. If, however, pressure recovery turns out to be important, a variable-area diffuser then should be employed.

Acknowledgments

This work has been supported by a research grant from the Rockwell International Foundation Corporation Trust and Contract N00014-85-K-0646 of the U.S. Navy Office of Naval Research.

References

[1]Ferri, A. and Edelman, R., "Some Observations on Heterogeneous Mixing Inside Channels," New York University, New York, Rept. NYU-AA-67-109, Aug. 1967.

[2]Bernstein, A., Heiser, W. H., and Hevenor, C., "Compound-Compressible Nozzle Flow," *Transactions of the ASME,* Vol. 34, Sept. 1967, pp. 548–554.

[3]Cosner, R. R., "Experiments on Thin Airfoils Spanning a Transonic Shear Flow," Ph.D. Thesis, California Institute of Technology, Pasadena, CA, June 1976.

[4]Papamoschou, D., "Experimental Investigation of Heterogeneous Compressible Shear Layers," Ph.D. Thesis, California Institute of Technology, Pasadena, CA, Dec. 1986.

[5]Papamoschou, D. and Roshko, A., "Observations of Supersonic Shear Layers," AIAA Paper 86-0162, Jan. 1986.

[6]Dutton, J C., Mikkelsen, C. D., and Addy, A. L., "A Theoretical and Experimental Investigation of the Constant-Area, Supersonic-Supersonic Ejector," *AIAA Journal,* Vol. 20, Oct. 1982, pp. 1392–1400.

Velocity Profile Model for Two-Dimensional Zero-Pressure Gradient Transitional Boundary Layers

H. Pfeil* and T. Müller†
Technische Hochschule Darmstadt, Darmstadt, Federal Republic of Germany

Received Jan. 8, 1988; revision received Aug. 15, 1988.

*Professor, Institute for Thermal Turbomachines.
†Research Engineer, Institute for Thermal Turbomachines.

Nomenclature

$A_{1,2,3,4}$ = constants of the law of the wall, Eq. (8)
C_T = universal additive constant of the logarithmic law of the wall, = 5
$C_1, \tilde{c}$ = constants of the law of the wall, Eq. (8)
C_{0T} = universal additive constant, Eq. (5)
f = function
H = shape parameter, $= \delta_1/\delta_2$
K = constant, Eq. (13)
m = exponent of Falkner Skan similarity solutions
Re_δ = Reynolds number based on boundary-layer thickness, $= U_\infty \delta/\nu$
Re_1 = Reynolds number based on displacement thickness, $= U_\infty \delta_1/\nu$
Re_2 = Reynolds number based on momentum thickness, $= U_\infty \delta_2/\nu$
Tu = freestream turbulence intensity, $= (\overline{u'^2}/U_0^2)^{0.5}$
u = mean velocity component parallel to the wall
u_{1m} = scaling velocity of the wake function
u_τ = friction velocity, $(\tau_w/\rho)^{0.5}$
u^+ = nondimensional mean velocity, $= u/u_\tau$
U_0 = freestream velocity
U_∞ = freestream velocity at the edge of the boundary layer
X = nondimensional characteristic quantity, $= |y^+ \kappa|_\delta = Re_\delta \omega \kappa$
y = local coordinate normal to the wall
y^+ = nondimensional wall distance, $= y u_\tau/\nu$
β = constant, here $\beta = \frac{3}{4}\pi^2$
δ = boundary-layer thickness
δ_1 = displacement thickness
δ_2 = momentum thickness
η = nondimensional wall distance, $= y/\delta$
κ = constant of the law of the wall, Eq. (8)
κ_T = von Kármán constant, = 0.41
Λ = nondimensional pressure gradient, $= (\delta^2/\nu)(dU_\infty/dx)$
ν = kinematic viscosity
ρ = fluid density
ω = nondimensional friction velocity, $= u_\tau/U_\infty$
Φ_1 = wake function
Φ_2 = law of the wall function
Φ_3 = correction function
τ_w = wall shear stress, $= \rho u_\tau^2$

Indices

a = outer region
i = inner region
I = instability point
L = laminar
P = Pohlhausen
Tr = transition point
T = turbulent
$T1$ = first turbulence profile after transition

I. Introduction

MEASURED turbulent boundary-layer profiles in a plane flow can be described with good agreement by the Coles profile model,[1] especially if the abrupt change in the slope at the outer edge of the boundary layer is eliminated, so that the velocity gradient $\partial u/\partial y|_\delta$ becomes zero.

$$\frac{u_T}{U_\infty} = 1 - \frac{\omega}{\kappa}[\Phi_2(\eta) - \Phi_3(\eta)] - \frac{u_{1m}}{U_\infty}\Phi_1(\eta)$$

$$= 1 - \frac{\omega}{\kappa}[-\ln(\eta) - (\tfrac{1}{2} - 3\eta^4 + 4\eta^5 - 1.5\eta^6)]$$

$$- \frac{u_{1m}}{U_\infty}\cos^2\left(\frac{\pi}{2}\eta\right) \qquad (1)$$

Equation (1) shows the Coles profile model with an additional correction term. The shape of the modification function Φ_3 chosen here is basically similar to the function $0.5\,\eta^2$. The shape of the modification function is of no great importance for the description of turbulent boundary-layer profiles as long as the velocity profile gradient vanishes at the outer edge. But, a higher order polynomial is used here so that the first three derivatives of the modification function vanish at the wall.

The profile model defined by Eq. (1) is not valid for the velocity distribution in the viscous sublayer near the wall. It can be shown that the Pohlhausen approximate equation[2] for laminar boundary layers can be rearranged in the following way [Eq. (2)], where, similarly to Eq. (1), it is divided into a law of the wall Φ_{2P} and a wake function Φ_{1P}:

$$\frac{u_L}{U_\infty}=1-\left(1-\frac{u_{1m}}{U_\infty}\right)[\Phi_{2P}(\eta)-\Phi_{3P}(\eta)] - \frac{u_{1m}}{U_\infty}\Phi_{1P}(\eta) \tag{2a}$$

$$\frac{u_{1m}}{U_\infty}=\frac{1}{2}-\frac{\Lambda}{24}=1-\frac{1}{4}Re_\delta\omega^2 \tag{2b}$$

$$\Phi_{1P}=1-6\eta^2+8\eta^3-3\eta^4 \tag{2c}$$

$$\Phi_{2P}-\Phi_{3P}=1-4\eta+6\eta^2-4\eta^3+\eta^4 \tag{2d}$$

Therefore, both laminar and turbulent boundary layers basically can be described both by a law of the wall and a superposed law of the wake. This makes it possible to develop a common velocity profile mode of laminar, turbulent, and also transitional two-dimensional boundary layers.

In Fig. 1, a laminar and a turbulent velocity profile are plotted in new coordinates $u^+\kappa=f(y^+\kappa)$ in contrast to the classical coordinates $u^+=f(y^+)$. The universal character of the logarithmic law of the wall

$$u^+=\frac{1}{\kappa_T}\ln(y^+)+C_T \tag{3}$$

is not influenced by this. Equation (3) is transformed in the following way:

$$u^+\kappa_T=\ln(y^+\kappa_T)+C_T\kappa_T-\ln(\kappa_T)=\ln(y^+\kappa_T)+C_{0T} \tag{4}$$

The new universal additive constant $C_{0T}=2.9416$ is calculated with the values $\kappa_T=0.41$ and $C_T=5.0$ as proposed by Coles.[3]

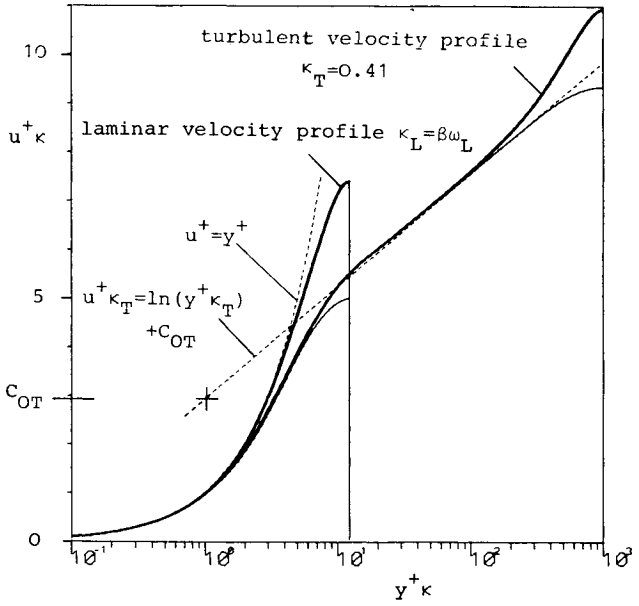

Fig. 1 Laminar and turbulent velocity profile according to Eqs. (7), (11), and (12), $\Lambda=0$

As a first approximation laminar boundary-layer profiles can be assumed to be a one parameter family of curves (local similarity). We then get for a nondimensional pressure gradient Λ:

$$u_L/U_\infty=f(\eta) \tag{5}$$

Replacing κ_L by $\beta\omega_L$ in the description $u^+\kappa=f(y^+\kappa)$ leads to identical agreement with the similarity equation, Eq. (5), provided that the velocity profiles of laminar boundary layer depend on the nondimensional pressure gradient Λ.

Measurements of zero-pressure gradient transitional boundary layers were evaluated using different values of β. The best agreement was found for $\beta=\frac{3}{4}\pi^2$, but good results also were obtained for smaller values down to $\beta=1$. A final decision concerning the value of β may be possible when transitional boundary layers with pressure gradient are evaluated.

$$u^+\kappa_L=\beta(u_L/U_\infty) \tag{6a}$$

$$y^+\kappa_L=\eta\beta\,Re_\delta\omega_L^2=\eta f(\Lambda) \tag{6b}$$

where $y^+\kappa$ is not only considered to be the responsible nondimensional length scale of the velocity distribution $u^+\kappa$ for two-dimensional laminar and turbulent boundary layers but also for transitional boundary layers, where κ rises during transition from $\kappa=\kappa_L=\beta\omega_L$ to $\kappa=\kappa_T=0.41$. It is one subject of this investigation to examine the development of κ within the transition region by evaluating measured velocity profiles of transitional boundary layers. It is necessary for this investigation to use a law of the wall that satisfies the boundary conditions at the wall and fits the measured velocity distribution near the wall.

II. Law of the Wall

The law of the wall proposed here is a modified form of that of H. Pfeil and W. Sticksel[4]:

$$u_i^+\kappa=\ln(1+A_1y^+\kappa)+C_1[1-e^{-A_2y^+\kappa}(1+A_3y^+\kappa)] + A_4(y^+\kappa)^2(1+y^+\kappa)e^{-y^+\kappa}-\tilde{c}(3\eta^4-4\eta^5+1.5\eta^6) \tag{7a}$$

$$A_4=-0.5\frac{1}{X^2}\frac{\kappa}{\omega}\left(\Lambda+\frac{\pi^2}{2}\frac{u_{1m}}{U_\infty}\right) \tag{7b}$$

$$\tilde{c}=\left\{\frac{A_1X}{1+A_1X}+C_1X[A_2+A_3(XA_2-1)]e^{-A_2X} - A_4X^2(X^2-2X-2)e^{-X}\right\} \tag{7c}$$

The coefficients A_1, A_2, A_3, and C_1 are calculated by simultaneously solving the nonlinear set of Eqs. (8):

$$1=A_1+C_1(A_2-A_3) \tag{8a}$$

$$0=A_1^2+C_1A_2(A_2-2A_3) \tag{8b}$$

$$0=2A_1^3+C_1A_2^2(A_2-3A_3) \tag{8c}$$

$$0=C_1-C_T\kappa_T+\ln(\kappa_TA_1) \tag{8d}$$

These coefficients depend only on the von Kármán constant κ_T and the universal additive constant of the law of the wall C_T. For the values of κ_T and C_T normally used, A_1, A_2, A_3 and C_1 are shown in Table 1.

Table 1 Constants A_1, A_2, A_3, and C_1 of the law of the wall

	κ_T	C_T	A_1	A_2	A_3	C_1
Nikuradse[5]	0.4	5.5	0.5642	0.4346	0.3166	3.6887
Coles[3]	0.41	5.0	0.5816	0.4541	0.3339	3.4836

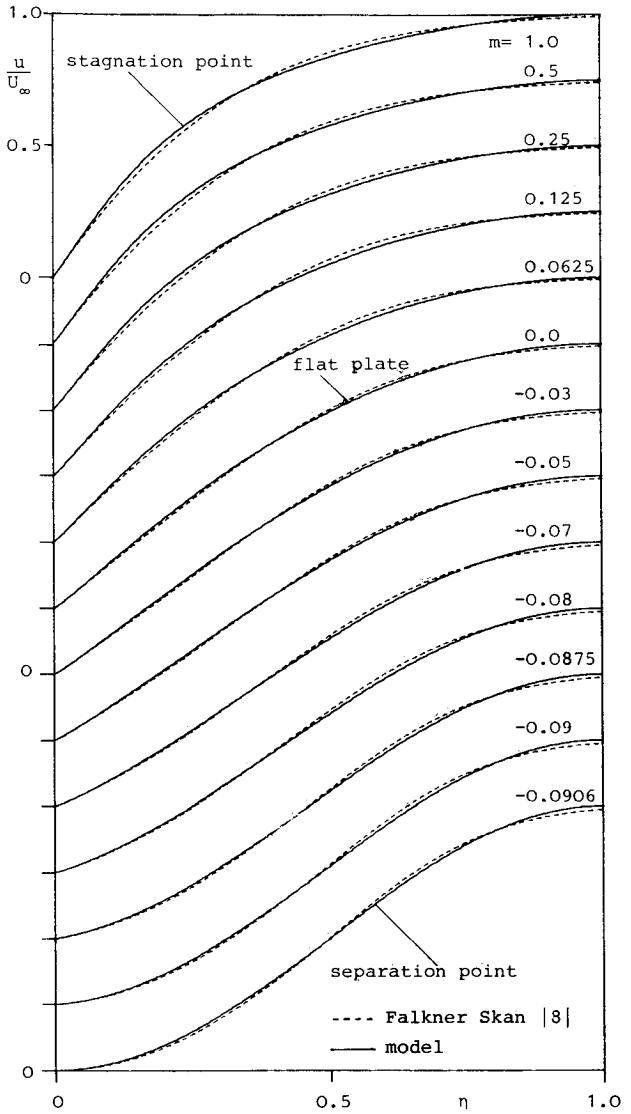

Fig. 2 Falkner-Skan similarity solution profiles compared with laminar velocity profiles according to Eqs. (11) and (12).

The following boundary conditions at the wall and at the outer edge are valid not only for laminar and turbulent but also for transitional boundary layers. These boundary conditions are satisfied by the complete velocity profile model formulated in Eq. (11).

$$\left.\frac{\partial(u^+\kappa)}{\partial(y^+\kappa)}\right|_{y^+\kappa=0}=1 \tag{9a}$$

$$\left.\frac{\partial^2(u^+\kappa)}{\partial(y^+\kappa)^2}\right|_{y^+\kappa=0}=-\Lambda\frac{\kappa}{\omega}\frac{1}{X^2} \tag{9b}$$

$$\left.\frac{\partial^3(u^+\kappa)}{\partial(y^+\kappa)^3}\right|_{y^+\kappa=0}=0 \tag{9c}$$

$$\left.\frac{\partial(u^+\kappa)}{\partial(y^+\kappa)}\right|_{(y^+\kappa)_\delta}=0 \tag{9d}$$

The scaling factor of the wake function, u_{1m}/U_∞ in A_4, satisfies the second derivative of the law of the wake at the wall. For $\kappa=\kappa_T$, the first line of Eq. (7a) represents the law of the wall for a turbulent flow over a flat plate without pressure gradient ($\Lambda=0$). This part of Eq. (7a) can be replaced by any one of the more than 40 proposed laws of the wall,[6] but only some of them fulfill the boundary conditions shown in Eqs. (9a–9c). The term multiplied by the factor A_4 in Eqs. (7a) satisfies the boundary condition introduced in Eq. (9b). This term cannot be derived and is therefore empirical, but it affects neither the theortical velocity distribution near the wall ($y^+\leq 5$) nor the logarithmic law of the wall ($y^+\geq 30$). Even for the greatest observed values of Λ in turbulent boundary layers[3] as well as in laminar boundary layers, the differences between the velocity distributions with and without this term are negligible. This term serves only as an alibi to satisfy the boundary condition [Eq. 9b)]. It is therefore omitted in the following considerations.

III. Law of the Wake

The law of the wake in this velocity profile model is the well-known wake function used by Hinze[7]:

$$\frac{u_a}{U_\infty}=\frac{u_{1m}}{U_\infty}[1-\Phi_1(\eta)]=\frac{u_{1m}}{U_\infty}\left(1-\cos^2\left[\frac{\pi}{2}\eta\right]\right) \tag{10}$$

IV. Velocity Profile Model

The complete profile model is a superposition of the law of the wake and the law of the wall:

$$\frac{u}{U_\infty}=f\left(\frac{\omega}{\kappa},X,\frac{u_{1m}}{U_\infty},\eta\right)=1$$

$$-\frac{\omega}{\kappa}[\Phi_2(\eta)-\Phi_3(\eta)]-\frac{u_{1m}}{U_\infty}\Phi_1(\eta)$$

$$=1-\frac{\omega}{\kappa}\left\{-\ell n\frac{1+A_1X\eta}{1+A_1X}+C_1[(1+A_3X\eta)e^{-A_2X\eta}\right.$$

$$\left.-(1+A_3X)e^{-A_2X}]+\tilde{c}\left[\frac{1}{2}-3\eta^4+4\eta^5-1.5\eta^6\right]\right\}$$

$$-\frac{u_{1m}}{U_\infty}\cos^2\left(\frac{\pi}{2}\eta\right) \tag{11}$$

The validity of the Coles profile model for turbulent boundary-layer velocity profiles has been confirmed frequently in the past. For turbulent boundary layers, the model presented here is nearly identical with the Coles profile model so that a verfication is not necessary.

Applied to laminar boundary layers, the velocity profile model, Eq. (11), together with the momentum equation, Eq. (12a), and the energy equation, Eq. (12b), permits the calculation of two-dimensional incompressible laminar boundary layers:

$$\omega^2=\frac{d\delta_2}{dx}+(2+H)\delta_2U_\infty\frac{dU_\infty}{dx} \tag{12a}$$

$$\frac{d}{dx}(U_\infty^3\delta_3)=2\nu\int_0^\delta\left(\frac{\partial u}{\partial y}\right)2dy \tag{12b}$$

The laminar velocity profiles computed with this approximate method are compared with the Falkner-Skan[8] similarity solutions (Fig. 2) for the laminar boundary layer of a wedge flow.

When the calculation scheme is used to calculate the development of the laminar boundary layer of a cylinder in

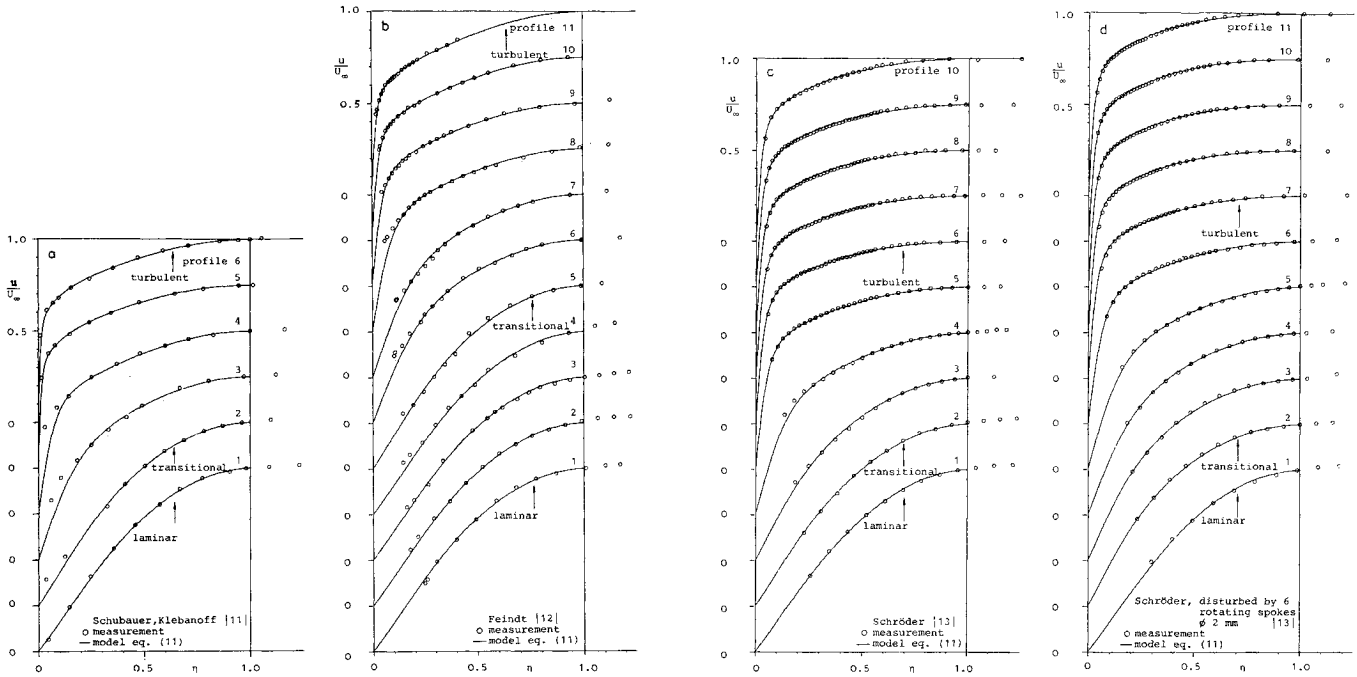

Fig. 3 Comparison of measured laminar, transitional, and turbulent velocity profiles with the model according to Eqs. (11-13).

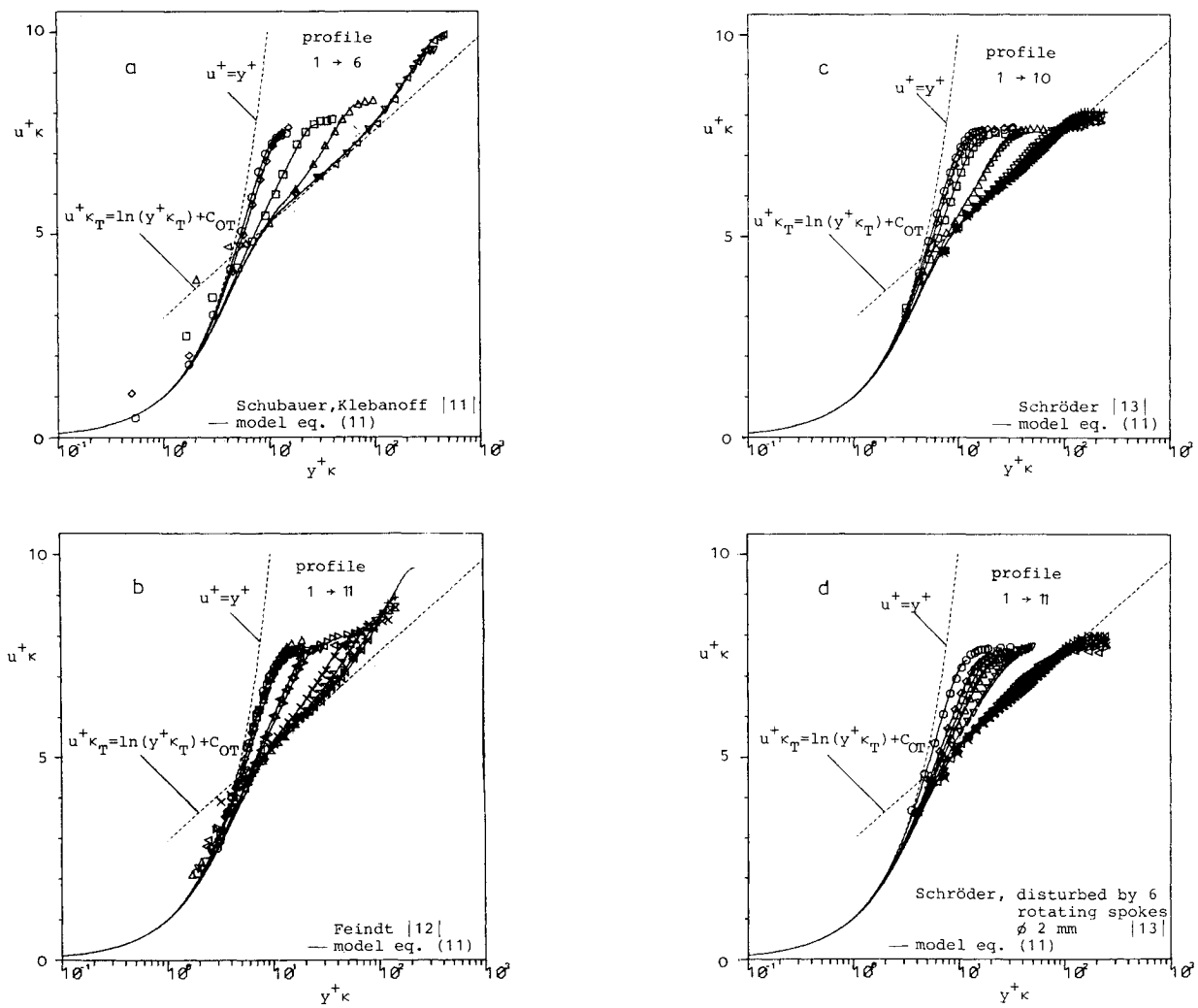

Fig. 4 Comparison of measured laminar, transitional, and turbulent velocity profiles with the model according to Eqs. (11-13).

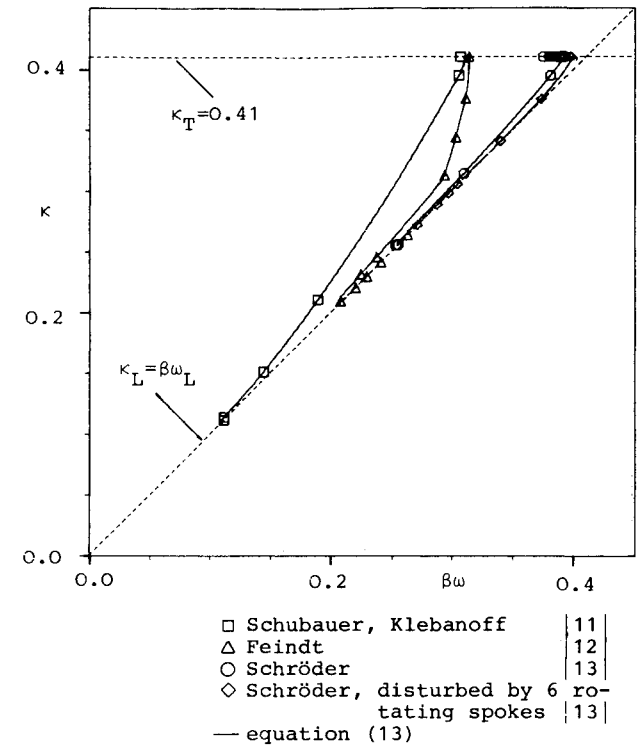

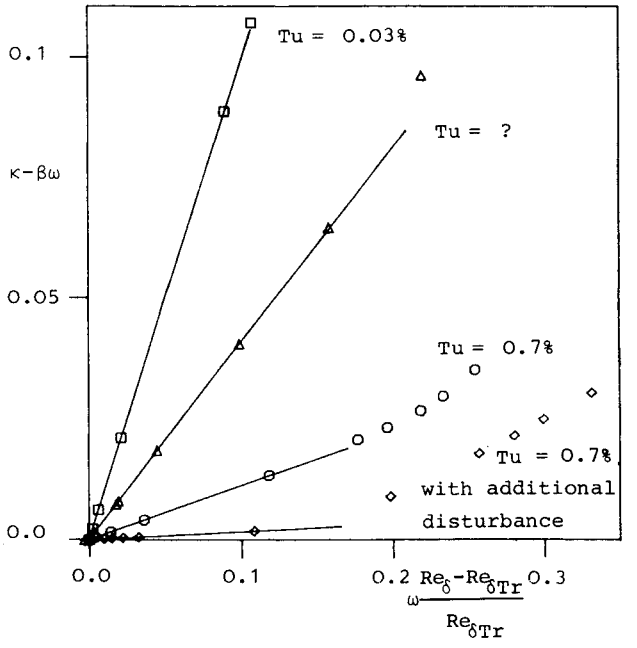

Fig. 5 Development of κ through the transition region according to Eq. (13).

crossflow, the resulting boundary-layer quantities show a good agreement with the exact numerical solutions calculated by Schönauer[9] until shortly before separation. Separation is predicted at 105.8 deg, whereas the exact solution is 104, 5 deg (Schönauer,[9] Terrill[10]).

V. Transitional Velocity Profile

Before Eq. (11) can be used to describe velocity profiles in transitional boundary layers, the development of κ within the transition region, where it rises from $\kappa=\beta\omega_L$ to $\kappa=\kappa_T=0.41$, has to be known. Although the velocity profile model defined by Eq. (11) permits a description of boundary layers of any pressure gradient, the following investigation deals only with constant pressure boundary layers. Measured velocity profiles of Schubauer and Klebanoff,[11] Feindt,[12] and Schröder[13] (two series) are used to determine the progress of κ in the transition region. The values of δ, u_{1m}/U_∞, and κ are varied until the best possible agreement of the velocity distribution given by Eq. (11) with the measured velocity profiles is found. In Figs. 3a–3d, the results of this fit are shown in the form $u/U_\infty=f(\eta)$, and in Figs. 4a–4d in the form $u^+\kappa=f(y^+\kappa)$.

Evaluation of the measured velocity profiles with the profile model [Eq. (11)] yields the relationships between κ, ω and Re_δ that are shown in Figs. 5a and 5b. This leads to the following equation describing the development of κ through the transition region.

$$\kappa-\beta\omega=K\omega\frac{Re_\delta-Re_{\delta Tr}}{Re_{\delta Tr}} \tag{13a}$$

$$K=1.65\left(1-\sqrt{\frac{Re_{\delta I}}{Re_{\delta Tr}}}\right) \tag{13b}$$

where $Re_{\delta I}=1194$, corresponding to $Re_{1I}=420$.

It is remarkable that κ is proportional to ω in the first part of the transition region, as shown in Fig. 5a. This proportionality is valid the longer the earlier transition occurs.

In this context it is interesting to compare the results for the first fully developed turbulent profile after transition with the results of Erm et al.,[14] who produced low Reynolds number turbulent boundary layers by forcing an early transition with stimulation pins. When the height of the stimulation pins was reduced, he observed that the Reynolds number based on the momentum thickness Re_{2T1} of the first respective turbulent profile increased ($Re_{2T1}=617, 672, 1359, 2425$). Similarly, the measurements evaluated here show that a reduced level of freestream turbulence, resulting in a delayed onset and completion of transition, also leads to an increase of Re_{2T1}. This observation is therefore well described by Eq. (13).

Table 2 shows the relations between the boundary-layer quantities of the first fully turbulent profile after transition and the Reynolds number Re_{2Tr} at the onset of transition.

Table 2 Boundary-layer quantities at the transition point and of the first fully developed turbulent profiles after transition

	Tu, %	Re_{2Tr}	Re_{2T1}	H_{T1}	ω_{T1}/ω_{Tr}
Schröder[13]	0.7, add. disturbed	164	432	1.502	1.463
Schröder[13]	0.7	185	467	1.493	1.540
Feindt[12]	?	289	1426	1.473	1.537
Schaubauer, Klebanoff[11]	0.03	965	2548	1.380	2.753

VI. Conclusion

A correlation was found to describe laminar, transitional, and turbulent boundary-layer profiles and is defined by Eqs. (11–13). These equations permit not only the evalution of measurements in transitional boundary layers in order to determine the skin friction but also more exact calculations of the displacement thickness δ_1 and the momentum thickness δ_2.

If the beginning of transition is known as a function of freestream turbulence intensity (for example, Granville[15]), the development of transition is described by Eq. (13). It also is possible to calculate intermittency and shear-stress distributions in transitional boundary layers. Equation (13) was determined by evaluating constant pressure boundary layers. The next step is to evaluate boundary layers with non-zero pressure

gradients in order to check the validity of Eq. (13) for these cases as well.

Acknowledgment

The authors would like to thank the Deutsche Forschungsgemeinschaft (DFG) for supporting the work described in this paper.

References

[1]Coles, D. E., "The Law of the Wake in the Turbulent Boundary Layer," *Journal of Fluid Mechanics,* Vol. 1, Feb. 1956, pp. 191–226.

[2]Pohlhausen, K., "Zur näherungsweisen Integration der Differentialgleichung der laminaren Reibungsschicht," *Zeitung für angewandte Mathematik und Mechanik,* Vol. 1, June 1921, pp. 252–268.

[3]Coles, D. E. and Hirst, E. A., "Computation of the Turbulent Boundary Layers," *Proceedings of the 1968 AFOSR-IFP-Stanford Conference,* Vol. II, Compiled Data, Stanford Univ., Stanford, CA, 1969.

[4]Pfeil, H. and Sticksel, W. J., "Influence of the Pressure Gradient on the Law of the Wall," *AIAA Journal,* Vol. 20, March 1982, pp. 434–436.

[5]Nikuradse, J., "Gesetzmäßigkeiten der turbulenten Strömung in glatten Rohren," *VDI–Forschungsheft* 356, Vol. 3, Sept. 1932.

[6]Coantic, M., "Contributions á l'etude de la structure de la turbulence dans une conduite circulaire," Dissertation, University d'Aix-Marseilles, France, 1966.

[7]Hinze, J.O., *Turbulence,* McGraw-Hill, New York, 1959.

[8]Falkner, V. M. and Skan S. W., Solution of the Boundary Layer Equations," *The London Edinburgh and Dublin Philosophical . Magazine and Journal of Science* 7th Ser., Nov. 1931, p. 865.

[9]Scönauer, W., "Ein Differenzenverfahren zur Lösung der Grenzschichtglei-chungen für stationäre, laminare, inkompressible Strömung," *Ingenieurarchiv,* Vol. 33, June 1964, p. 173.

[10]Terrill, R. M., "Laminar Boundary-Layer Flow Near Separation With and Without Suction," Vol. 253, No. 1, 1960, p. 55.

[11]Schubauer, G. B. and Klebanoff, P. S., "Contributions on the Mechanics of Boundary-Layer Transition," NACA Report 1289, Feb. 1955.

[12]Feindt, E. G., "Untersuchung über die Abhäqngigkeit des Umschlages laminar-turbulent von der Oberflächenrauhigkeit und der Druckverteilung," Dissertation, TH Braunschweig, Institut für Strömungsmechanik, FRG, 1956.

[13]Schröder, T., "Entwicklung des instationären Nachlaufs hinter quer zur Strömungsrichtung bewegten Zylindern und dessen Einfluß auf das Umschlagverhalten von ebenen Grenzschichten stromabwärts angeordneter Versuchskörper," Dissertation, TH Darmstadt, Institut für Thermische Turbomaschinen, FRG, 1985.

[14]Erm, L. P., Smits, A. J., and Joubert, P. N., "Low Reynolds Number Turbulent Boundary Layers on a Smooth Flat Surface in a Zero Pressure Gradient," *Turbulent Shear Flow,* F. Durst, B. E. Launder, J. L. Lumley, F. W. Schmidt, and J. H. Whitelaw, Springer-Verlag, Berlin.

[15]Granville, P. S., "The Calculations of Viscous Drag of Bodies of Revolution," U.S. Navy, Report 849, 1953. David Taylor Model Basin.

Mass Transfer in a Binary Gas Jet

J. Y. Zhu,* R. M. C. So,† and M. V. Ötügen‡
Arizona State University, Tempe, Arizona

Introduction

TURBULENT gas jets have been investigated extensively in the past because of their intrinsic importance to the study of supersonic and hypersonic flows, combustor performance, geophysical flows, and variable-density mixing phenomena. In most of the earlier investigations, measurements were limited to the jet growth rate, centerline decay behavior, and similarity scaling parameters.[1] With the advent of hot-wire anemometry, hot-wire type concentration probes were developed to measure the concentration field alone[2,3] and to measure the concentration and velocity fields simultaneously.[4,5] Later, these probes were used to study the density field in a two-dimensional mixing layer of helium and nitrogen[3] and to measure velocity and helium volume concentration simultaneously in a helium/air mixture.[5] The latter study was able to demonstrate that some of the turbulent mass flux terms normally neglected in the jet equations were not small compared to those mass flux terms that were retained in the equations. Since detailed measurements of the mixing process were not made, the behavior of mass transfer in a variable-density flow was not studied.

Alternatives to hot wires are optical techniques. Batt[6] proposed the use of a fiber-optic probe to measure species concentration whereas Raman and Rayleigh scattering techniques were developed by Birch et al.[7] and Pitts and Kashiwagi.[8] These techniques were far better than the hot-wire probe[4] because the concentration measurements were independent of velocity, and they can be integrated easily with laser Doppler anemometry (LDA) to measure concentration simultaneously with velocity. Even though LDA/Raman and LDA/Rayleigh techniques have not been used to study binary mixing, the two techniques have been applied to examine premixed[9,10] and nonpremixed[11] flames. These studies led to an understanding of mass transfer in flames and showed that, because of heat-release effects, the gradient diffusion assumption that was commonly made to model turbulent axial mass flux was not valid.[11] In spite of these advances, mass transfer in isothermal, binary mixing is still little understood.

Since the hot-wire type concentration probe[2] measures species concentration independent of upstream velocity, it can be used with LDA to measure velocity and concentration simultaneously. Zhu et al.[12] took advantage of this fact and developed a laser/hot-wire technique to do just that. As a result, a simple technique is now available for the study of mass transfer in binary gas jets. This Note presents the results of an attempt to use the laser/hot-wire technique[12] to measure velocity and concentration simultaneously in the developing region of a free binary gas jet.

Experimental Setup

The jet test rig consisted of a cylindrical plenum fitted with a well-contoured convergent nozzle at one end of the cylinder. The cylindrical plenum was 304.8 mm in depth and 132.4 mm in diameter, while the jet nozzle diameter (D) was 9.5 mm. A honeycomb section of 127 mm in length installed just ahead of the convergent nozzle was used to straighten the flow and to destroy the large eddies inside the plenum. Premixed helium/air mixture with 50% of helium by volume was delivered to the plenum from compressed gas bottles. A DISA Model 55L18 seeding generator capable of generating liquid droplets (50% water and 50% glycerine), centered around 1 μm in size, was connected to the plenum. Since the liquid droplets were carried into the plenum by an air stream, the resultant helium/air mixture delivered to the jet had a helium volume concentration of $<50\%$ depending on the droplet concentration required for accurate LDA measurements of the jet velocity field. Once the right droplet concentration was determined, the supply pressures of the seeding generator air stream and the helium/air mixture were fixed and maintained constant for the whole experiment. Consequently, a fairly constant jet plenum condition was obtained, and the jet velocity and helium volume concentration were quite uniform at the jet nozzle exit. The whole facility was arranged vertically so

Received Jan. 4, 1988; revision received May 6, 1988; presented as Paper 88-3813 at the 1st National Fluid Dynamics Congress, Cincinnati, OH, July 25–28, 1988.

*Graduate Assistant, Mechanical and Aerospace Engineering Department.

†Professor, Mechanical and Aerospace Engineering Department

‡Research Associate, Mechanical and Aerospace Engineering Department.